

# MR evaluation of tongue carcinoma in the assessment of depth of invasion with histopathological correlation: A single center experience

Reddy Ravikanth

Department of Radiology, Holy Family Hospital, Thodupuzha, Kerala, India

**Correspondence:** Dr. Reddy Ravikanth, Department of Radiology, Holy Family Hospital, Thodupuzha - 685 605, Kerala, India.  
E-mail: ravikanthreddy06@gmail.com

## Abstract

**Introduction:** Magnetic resonance imaging (MRI) has become the cornerstone for pretreatment evaluation of carcinoma tongue and provides accurate information regarding the extent of the lesion and depth of invasion that helps the clinician to optimize treatment strategy. Aim of the study is to correlate MRI and histopathological findings, to evaluate the role of MRI in loco-regional tumor node metastasis (TNM) staging, and to assess the depth of invasion of tongue carcinoma. **Materials and Methods:** This study was undertaken on 30 patients with clinical diagnosis of tongue carcinoma referred for MR imaging at a tertiary care hospital over the 2-year period between July 2017 and June 2019. MRI was performed with GE 1.5 Tesla scanner, neurovascular (NV) array coil. Clinical and MRI staging of tongue carcinoma was done preoperatively and correlated. Post-surgery, histopathological TNM staging was done and correlated with clinical and MRI TNM staging. The cutoff value of histopathological (HP) depth that could determine the existence of nodal metastasis was 5 mm. **Results:** In 30 patients diagnosed with tongue carcinoma, the incidence was higher in males (92%). Moderate agreement ( $k = 0.512$ ) was noted for T staging between clinical and MRI staging assessments. Fair agreement ( $k = 0.218$ ) was noted for N stage between clinical and MRI staging assessments. There was good agreement ( $k = 0.871$ ) for M stage between the clinical and MRI staging assessments. Good agreement ( $k = 0.822$  and  $k = 0.767$ , respectively) was noted for both T staging and N staging between MRI and histopathology staging assessments. The agreement for the T stage was poor ( $k = 0.012$ ) between the clinical and histopathology staging assessments. Agreement for the N stage was also poor ( $k = 0.091$ ) between the clinical and histopathology staging assessments. Mean depth of invasion by histology and MRI was 14.22 mm and 16.12 mm, respectively. Moderate agreement ( $k = 0.541$ ) was noted between clinical and pathological tumor depth and good agreement ( $k = 0.844$ ) was noted between radiological and pathological tumor depth. As for the T1WGd MRI depth with a cutoff value of 5 mm, the nodal metastasis rate in the group with values  $>5$  mm was 52%, and for those  $<5$  mm was 24%, both of which were significantly different ( $P = 0.040$ ). Pearson's correlation coefficient of HP depth and T1WGd MRI depth was 0.851 ( $P < 0.001$ ) suggesting that HP depth shows a strong correlation with T1WGd MRI depth. **Conclusion:** MRI is the imaging modality of choice for evaluation of tongue carcinoma as MRI helps in accurate staging of the tumor using TNM classification which is crucial for optimizing treatment options. The current study shows a high correlation between MRI and histopathological findings regarding thickness of tumor and depth of invasion. MRI and histopathology assessments of tumor spread were equivalent

This is an open access journal, and articles are distributed under the terms of the Creative Commons Attribution-NonCommercial-ShareAlike 4.0 License, which allows others to remix, tweak, and build upon the work non-commercially, as long as appropriate credit is given and the new creations are licensed under the identical terms.

**For reprints contact:** WKHLRPMedknow\_reprints@wolterskluwer.com

**Cite this article as:** Ravikanth R. MR evaluation of tongue carcinoma in the assessment of depth of invasion with histopathological correlation: A single center experience. Indian J Radiol Imaging 2020;30:126-38.

**Received:** 08-Jul-2019  
**Accepted:** 10-Apr-2020

**Revised:** 08-Oct-2019  
**Published:** 13-Jul-2020

### Access this article online

#### Quick Response Code:



**Website:**  
www.ijri.org

**DOI:**  
10.4103/ijri.IJRI\_286\_19

to within 0.5 mm DOI. Estimation of invasion depth using MRI as a preoperative study in oral tongue carcinoma is essential in planning surgical treatment strategies such as the extent of elective neck dissection. Invasion depth, which greatly affects occult node metastases, must be included in the TNM staging of oral tongue carcinoma.

**Key words:** Depth of invasion; magnetic resonance imaging; tumor node metastasis staging; tongue carcinoma

## Introduction

Most tumors of the tongue occur on the lateral and under surface.<sup>[1]</sup> Dorsal tumors are uncommon but when they do occur, they are usually located near the midline and more posteriorly.<sup>[2]</sup> Oral tongue tumors tend to remain in the tongue. Tumors in the anterior third of the oral tongue invade the floor of the mouth.<sup>[3]</sup> Middle-third lesions infiltrate the musculature of the tongue and later, the lateral floor of the mouth.<sup>[4]</sup> Carcinomas involving the posterior third of the tongue grow into the musculature of the tongue, the floor of the mouth, the anterior tonsillar pillar, the tongue base, the glosso-tonsillar sulcus, and the mandible.<sup>[5]</sup>

MRI provides valuable information both within and without the tongue. The tongue carcinoma may extend far beyond the gross tumor margin seen on surgery, which is often deceiving. It is known that the most important factor governing local recurrence is the resection margin.<sup>[6]</sup> Whereas 1 cm is generally considered adequate for most squamous cell carcinomas, the margins for tongue cancer should be 1.5–2.0 cm.<sup>[7]</sup> Tumors with deep margins are often difficult to assess during surgery. In addition, these tumors are technically more difficult to resect. Hence, deep margins are frequently the site of positive or inadequate resection margins. Up to 35% of patients have nodal metastasis on presentation.<sup>[8]</sup> Five percent of these patients have bilateral lymph node involvement.<sup>[9]</sup> The first echelon nodes are the submandibular and jugulodigastric nodes.<sup>[10]</sup> Submental node involvement is uncommon except in patients with tumor at the tip of tongue.<sup>[11]</sup> It should be noted that in patients with clinically N0 neck, the overall occult metastatic rate is approximately 30%.<sup>[12]</sup> Various clinical studies have been performed to correlate the depth of tumor invasion with the likelihood of cervical nodal metastasis. These studies reveal that the single most important factor in predicting lymph node metastasis is the depth of tumor invasion.<sup>[13]</sup>

Tongue base carcinoma is a clinically silent region and tumors tend to spread with deep infiltration. As a general rule, the extent of these tumors is underestimated during clinical examination. Tongue base tumors tend to remain in the tongue except for laterally placed lesions or late cases. Under such circumstances, tongue base tumors may extend into the tonsillar fossa. Tonsillar carcinomas, on the other hand, have a tendency to invade the tongue base. For tongue base carcinoma, the first echelon nodes are the

jugulodigastric nodes, followed by mid and lower jugular nodes. Retropharyngeal nodes are occasionally involved. Submandibular nodes may be involved if there is anterior tumor extension. Submental nodes are rarely involved. Seventy-five percent of patients have positive nodes on presentation, while 30% have bilateral nodal metastases.<sup>[14]</sup> Patients with clinically N0 neck have a 30%–50% rate of occult metastases.<sup>[15]</sup>

## Imaging anatomy

The tongue comprises dorsum, apex, inferior surface, and root. The root (base) is attached to the hyoid bone and mandible while the apex forms the tip of the tongue. The sulcus terminalis is a shallow groove with the circumvallate papillae just anterior to it and divides the tongue into the oral (anterior two-thirds) and pharyngeal (posterior third) parts. As a general guide on axial imaging, a line joining the anterior aspect of the mandibular rami may be used as the dividing line between these two parts, which differ in their developmental origins and hence their nerve supplies.<sup>[16]</sup>

The tongue muscles are divided into intrinsic and extrinsic groups. The intrinsic muscles are entirely within the tongue with no bony attachment and are organized into superior and inferior longitudinal, vertical, and transverse bands. Their principle function is altering the shape of the tongue. The extrinsic muscles consist of genioglossus, hyoglossus, styloglossus, and palatoglossus. These extrinsic muscles stabilize the tongue and alter its position, as well as its shape. All the muscles of the tongue, intrinsic and extrinsic, are thus innervated by the hypoglossal nerve. The exception being palatoglossus, which being essentially a palate muscle, is supplied by the pharyngeal plexus.

The anatomy of the tongue is well demonstrated on magnetic resonance imaging (MRI). On axial T1-weighted images, fat with high signal intensity can be seen interspersed between the muscles of intermediate signal intensity. MRI is the preferred modality in the evaluation of tongue carcinomas. The abnormal signals seen on MRI are well correlated with pathological findings. Tumor invasion of the floor of the mouth is particularly well seen on coronal images. Sagittal images provide information on tongue base involvement and the extent of pharyngeal infiltration.<sup>[17]</sup>

Genioglossus is the largest of all the tongue muscles and forms the bulk of the tongue. It arises from the genial

tubercle and is easily seen on MRI. It fans out widely and inserts inferiorly into the hyoid bone; posteriorly into the tongue base; and superiorly into the entire ventral surface of the tongue. Hyoglossus is a thin quadrilateral sheet of muscle arising from the hyoid bone. It ascends superiorly, interdigitating with the fibers of the styloglossus, and attaches to the side of the tongue. The hyoglossus muscles define the lateral margins of the tongue and are readily identified on MRI. Both the styloglossus (which arises from the styloid process and stylohyoid ligament) and the palatoglossus (which originates from the palatine aponeurosis) cannot be seen with certainty on imaging studies. Lymph from the tip of the tongue drains to the submental nodes. Marginal lymphatics from the outer third of the rest of the oral tongue are directed to ipsilateral submandibular and jugulodigastric nodes. Central lymphatics of the inner two-thirds of the oral tongue have pathways to nodes of both sides of the neck.<sup>[18]</sup>

**TNM staging**

Tumor node metastasis (TNM) classification is the most commonly used system for describing malignant tumors, their regional involvement, and distant metastases.<sup>[19]</sup> The TNM and stage grouping are presented below:

**Aims and objectives**

Aim of the study is to correlate MRI and histopathological findings, to evaluate the role of MRI in loco-regional TNM staging, and to assess the depth of invasion of tongue carcinoma.

**Materials and Methods**

This study was undertaken in the Department of Radiology at a tertiary care hospital in India over the 2-year period between July 2017 and June 2019. Before subjects were recruited, the study protocol was approved by the institutional ethics committee (IEC), in accordance with the ethical principles for human investigation outlined by the Second Declaration of Helsinki, and written informed consent was obtained from all patients prior to their enrollment in this study (IEC, Holy Family Hospital; IEC Approval Reference Number: HFH/12/2017; IEC Approval Date: June 12, 2017). MR examinations were performed using a 1.5-T scanner (Signa, General Electric Medical Systems, Milwaukee, WI, USA). Neurovascular (NV) arraycoil was used. The patient’s head was secured using relaxing cushion; ensuring that the shoulders touch the lower part of the coil. The protocol included axial, sagittal, and coronal T1-weighted turbo spin echo (TSE), axial and coronal T2-weighted turbo spin echo (TSE), and gadolinium-enhanced axial and coronal T1-weighted sequences with fat suppression (FS) as well as diffusion-weighted (DW) sequences [Table 1]. The tumor depth was measured at post contrast T1 coronal

FS. The tumor thickness was defined by the distance from the deepest point of invasion to the tumor surface. At first, a vertical line joining the maximum length between tumor-mucosa junctions was drawn as a reference line. The tumor thickness was determined by the summation of two lines drawn perpendicular from the reference line to the point of maximum tumor extension.

Clinical and MRI staging of tongue carcinoma was done preoperatively and correlated [Figures 1-16]. Post-surgery, histopathological TNM staging was done and correlated with clinical and MRI TNM staging [Figures 17-20 and Tables 2-5]. T1 tumor measures ≤2 cm in greatest dimension with depth of invasion (DOI) ≤5 mm. T2 tumor measures ≤2 cm with DOI >5 mm. T3 tumor measures >2 cm and ≤4 cm with DOI >10 mm. T4a is moderately advanced local disease tumor >4 cm with DOI >10 mm. T4b is very advanced local disease with tumor invasion into the masticator space, pterygoid plates, or skull base, and/or tumor encases the internal carotid artery.

**Statistical analysis**

Descriptive statistics were reported using numbers and percentages for categorical variables. Analysis was done

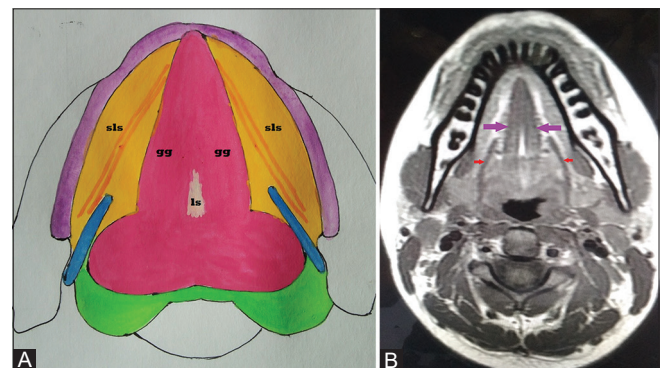


**Figure 1 (A and B):** Axial schematic representation (A) and T1-weighted magnetic resonance (MR) image (B) demonstrate the root of the tongue. The high-signal-intensity lingual septum (ls) is clearly seen and is flanked by the genioglossus muscles (gg), which form an inverted V anteriorly before blending into the intrinsic muscles of the mobile tongue. The sublingual spaces (sls) are lateral to the genioglossus and geniohyoid muscles and also show high T1 signal intensity. Axial T1-weighted image (B) shows the tongue muscles, genioglossus (long arrow), and hyoglossus (short arrow)

**Table 1: Protocol for MRI Tongue in the current study is as below**

Sequence	Slice	Slice thickness	Gap	Matrix
T1 Axial	29	4 mm	0.4 mm	512
T1 Coronal	23	4 mm	0.4 mm	512
STIR Coronal	23	4 mm	0.4 mm	256
T2 Fatsat Axial	29	4 mm	0.4 mm	512
T1 Fatsat Axial+C	23	4 mm	0.4 mm	512
T1 Fatsat Coronal+C	19	4 mm	0.4 mm	512
T1 Fatsat Sagittal+C	19	4 mm	0.4 mm	512



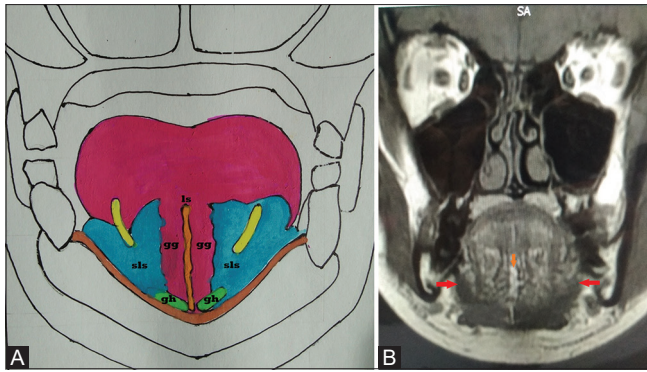


**Figure 2 (A and B):** Coronal schematic representation (A) and T1-weighted MR image (B) demonstrate genioglossus muscles (gg) which resemble paramidline vertical pillars. Below the genioglossus muscles, the geniohyoid muscles (gh) appear subtly wider than they do on axial images [Figure 1]. The sublingual spaces (sls) show high T1 signal intensity. ls = lingual septum. Coronal T1- weighted image (B) shows lingual septum (short arrow) and mylohyoid (long arrow), which form the floor of the mouth

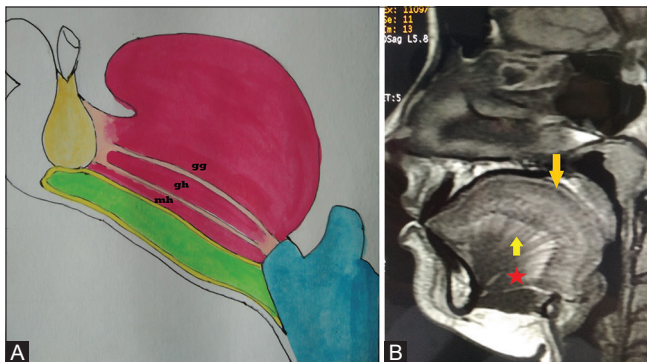


**Figure 3 (A and B):** Sagittal drawing (A) and T1-weighted MR image (B) demonstrate the geniohyoid muscles (gh) and the fanlike shape of the genioglossus muscles (gg). The mylohyoid muscle (mh) extends from the mandible to the hyoid bone and supports the floor of the mouth. Sagittal T1-weighted image (B) shows the fan-shaped genioglossus (short arrow), the longitudinal intrinsic muscle (long arrow), and darkly hypointense geniohyoid (star) from genial tubercle to hyoid

**Table 2: T-Primary tumor**

Stage	Status of primary tumor
TX	Primary tumor cannot be assessed
T0	No evidence of primary tumor
Tis	Carcinoma <i>in situ</i>
T1	Tumor 2 cm or less in greatest dimension
T2	Tumor more than 2 cm but not more than 4 cm in greatest dimension
T3	Tumor more than 4 cm in greatest dimension
T4a (lip)	Tumor invades through cortical bone, inferior alveolar nerve, floor of mouth, or skin (chin or nose)
T4a (oral cavity)	Tumor invades through cortical bone, into deep/extrinsic muscle of tongue (genioglossus, hyoglossus, palatoglossus, and styloglossus), maxillary sinus, or skin of face
T4b (lip and oral cavity)	Tumor invades masticator space, pterygoid plates, or skull base; encases internal carotid artery

**Table 3: N – regional lymph nodes**

Stage	Status of regional lymph nodes
NX	Regional lymph nodes cannot be assessed
N0	No regional lymph node metastasis
N1	Metastasis in a single ipsilateral lymph node, 3 cm or less in greatest dimension
N2	Metastasis as specified in N2a, 2b, 2c below
N2a	Metastasis in a single ipsilateral lymph node, more than 3 cm but not more than 6 cm in greatest dimension
N2b	Metastasis in multiple ipsilateral lymph nodes, none more than 6 cm in greatest dimension
N2c	Metastasis in bilateral or contralateral lymph nodes, none more than 6 cm in greatest dimension
N3	Metastasis in a lymph node more than 6 cm in greatest dimension

**Table 4: M – Distant metastasis**

Stage	Status of distant metastasis
MX	Distant metastasis cannot be assessed
M0	No distant metastasis
M1	Distant metastasis

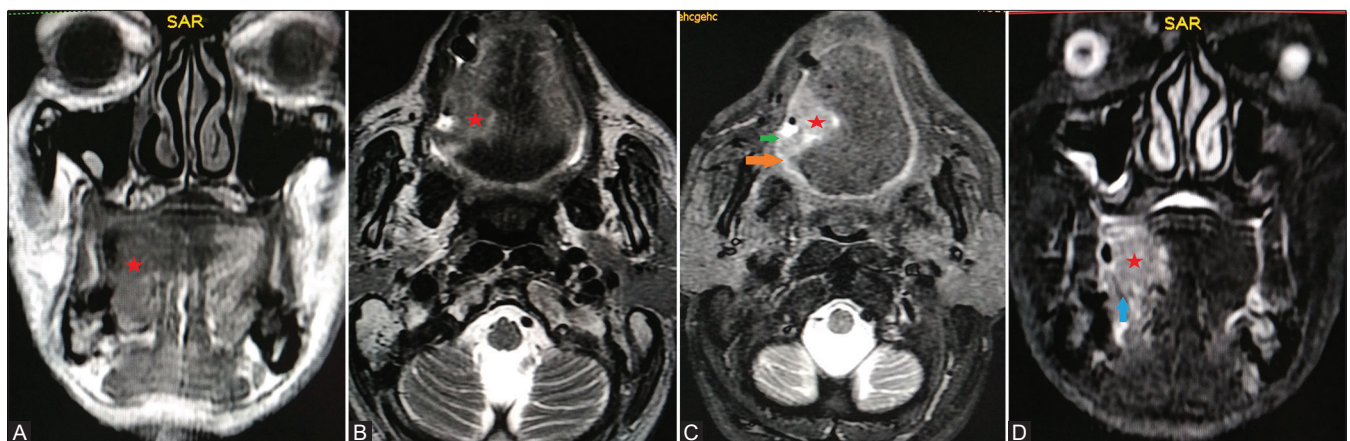


**Figure 4 (A-D):** Mass lesion (star) in the right lateral aspect of the anterior 2/3<sup>rd</sup> of the tongue with inferior extension into the posterior aspect of right sublingual space. The lesion appears isointense on T1 (A), hyperintense on T2 (B), and hyperintense on STIR (C and D) and extends medially up to the lingual septum with no obvious extension across the midline. Axial STIR image (C) demonstrates an ill-defined nodular mass lesion involving intrinsic muscles of the anterior tongue including genioglossus, mylohyoid, and geniohyoid. Inferiorly, the lesion invades the right lateral floor of mouth and sublingual space (short arrow). Posteriorly, there is an invasion of right pterygomandibular raphe (long arrow)



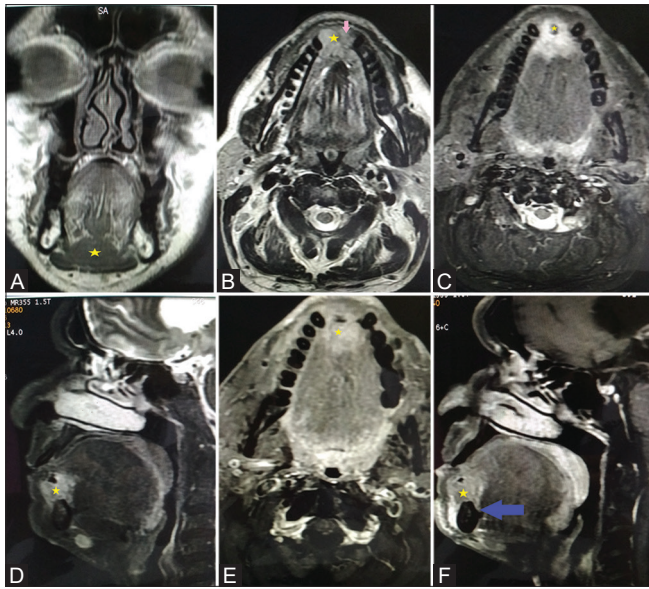


**Figure 5 (A-F):** Mass lesion (star) involving the alveolar margin of the mandible in the midline extending along the lingual septum and genioglossus muscle with infiltration of the sublingual spaces anteriorly. The lesion appears isointense on T1 (A), heterogeneously hyperintense on T2 (B), and hyperintense on STIR (C and D) showing contrast enhancement on T1 + c images (E and F) and a central focus of nonenhancement— suggestive of necrosis. Axial T2 weighted fat-suppression MR image (B) demonstrates a bulky enhancing tumor in genioglossus of anterior tongue extending into anterior alveolar margin of mandible causing erosion of occlusal cortices of mandible and enhancement in the marrow (short arrow). Sagittal T1 + c image (F) shows tumor invading the floor of the mouth (long arrow). There is sparing of the mylohyoid muscle inferiorly

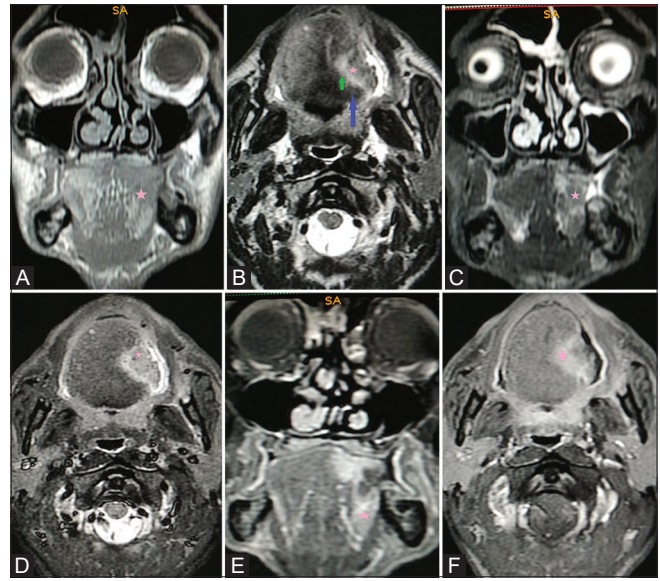


**Figure 6 (A-F):** Irregular shaped mass lesion (star) in the lateral aspect of the anterior 2/3<sup>rd</sup> of the left tongue with no extension across the midline and no obvious involvement of the floor of the mouth/sublingual space. The lesion appears isointense on T1 (A), heterogeneously hyperintense on T2 (B), and hyperintense on STIR (C and D) showing contrast enhancement on T1 + c images (E and F) with a central focus of nonenhancement—s/o necrosis. Axial T2 weighted fat-suppression MR image (B) demonstrates a nodular mass lesion in the anterior 2/3<sup>rd</sup> of the oral tongue with infiltration of the genioglossus (short arrow) and reaching up to sublingual space invading mylohyoid (long arrow). Coronal T1 + c image (E) shows no obvious invasion of the floor of mouth

using Microsoft Excel 2013, Microsoft Corp., Redmond, WA, USA and SPSS Statistical Package Version 20.0, IBM Corp., Armonk, New York, USA. *P* value (<0.05) was considered statistically significant. The inter-observer agreement was assessed using Kappa statistics.

**Results**

This study was undertaken on 30 patients with clinical diagnosis of tongue carcinoma referred for MR imaging at a tertiary care hospital over the 2-year period. 68% of the patients belonged to age group of 51–60 years, which was followed by the age group of 41–50 years comprising of 18% of the patients and 61–70 years comprising 13% of the patients. The incidence of oral cancers is higher in males constituting 92% of total patients. There was moderate agreement ( $k = 0.612$ ) for the T stage between the clinical and MRI staging assessments [Table 6] and fair agreement ( $k = 0.218$ ) for N stage between MRI and clinical staging assessments [Table 7]. Good ( $k = 0.822$ ) agreement for the T stage was seen between MRI and histopathology staging assessments [Table 8] and for N stage ( $k = 0.931$ ) between MRI and histopathology staging assessments [Table 9]. There was good agreement ( $k = 0.871$ ) for M stage between the clinical and MRI staging assessments. The agreement for the T stage was poor ( $k = 0.012$ ) between the

**Table 5: Stage grouping**

Group	Primary tumor	Regional lymph nodes	Distant metastasis
Stage 0	Tis ( <i>in-situ</i> )	N0	M0
Stage I	T1	N0	M0
Stage II	T2	N0	M0
Stage III	T3	N0	M0
	T1, T2, T3	N1	M0
Stage IVa	T4a	N0, N1	M0
	T1, T2, T3, T4a	N2	M0
Stage IVb	T4b	Any N	M0
	Any T	N3	M0
Stage IVc	Any T	Any N	M1

**Table 6: Correlation between MRI and clinical tumor (T) staging**

Clinical "T" staging	MRI "T" staging				Total
	T1	T2	T3	T4	
T1	1	0	0	0	1
T2	0	6	2	0	8
T3	0	3	6	2	11
T4	0	1	4	5	10
Total	1	10	12	7	30
Sensitivity					90.1%
Specificity					93.8%
PPV					95.0%
Kappa coefficient					0.612, 95% CI (0.521-1.00)

By applying the Chi-square test and kappa statistics, *P* and *k* come out to be 0.01 and 0.512, respectively, showing moderate agreement between the clinical and MRI staging assessments



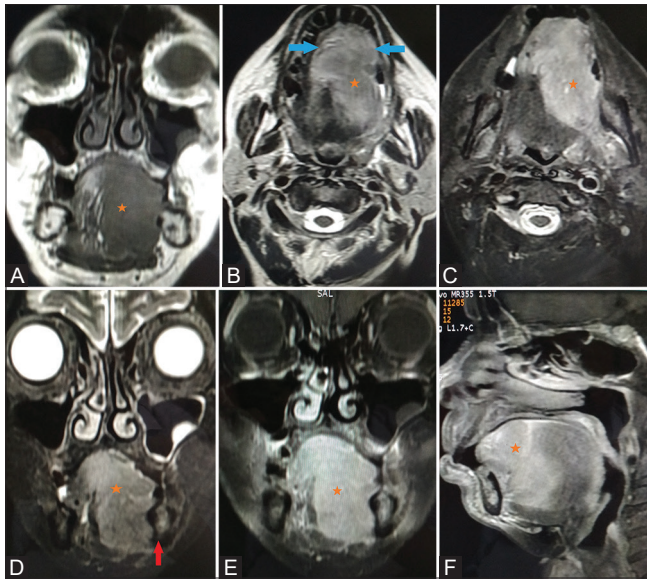


**Figure 7 (A-F):** Ill-defined mass lesion (star) extending along the anterior and left alveolar margins of the mandible with infiltration of bilateral genioglossus muscles, the lingual septum, bilateral sublingual spaces, left masticator space, left submandibular gland, and left geniohyoid muscle inferiorly. The lesion appears isointense on T1 (A), hyperintense on T2 (B), and hyperintense on STIR (C and D) showing contrast enhancement on T1 + c images (E and F). There is sparing of the mylohyoid muscle. Axial T2-weighted fat-suppression image (B) reveals an ill-defined heterogeneous signal intensity nodular mass lesion involving the anterior tongue on left side. It crosses midline anteriorly and involves genioglossus and geniohyoid. Coronal STIR image (D) shows tumor infiltration of the floor of the mouth. Note the involvement of ipsilateral mylohyoid muscle (short arrow) and normal contralateral mylohyoid. Note the tumor infiltration into bilateral sublingual glands (long arrows) on T2FS axial image (B)

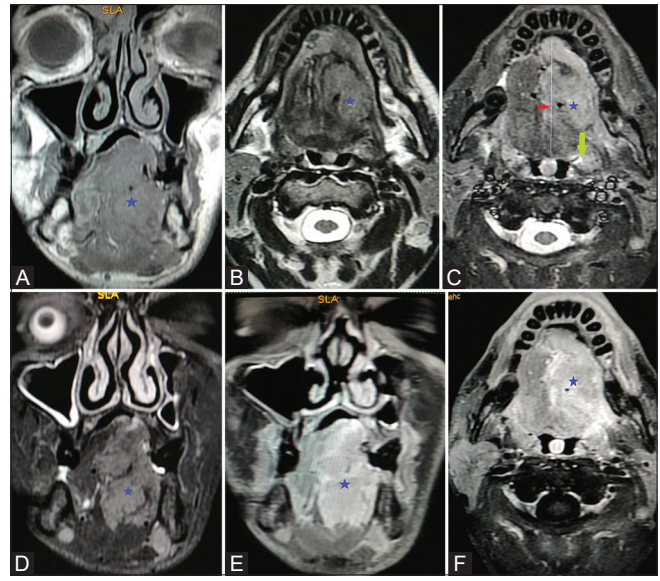


**Figure 8 (A-F):** Irregular shaped mass lesion (star) in the left side of the tongue appearing isointense on T1 (A), heterogeneously hyperintense on T2 (B), and hyperintense on STIR (C and D) showing contrast enhancement on T1 + c images (E and F). The lesion extends across the midline into the right side. Inferiorly the lesion extends into the left sublingual space causing loss of fat plane with the mylohyoid muscle and to the anterior aspect of the right sublingual space. Axial STIR image (C) demonstrates an ill-defined nodular hyperintense mass lesion of tongue invading genioglossus, mylohyoid, and geniohyoid in the left lateral and anterolateral aspects of the tongue extending up to lingual septum (short arrow) and crossing the midline (white line). Posteriorly, the lesion invades the base of tongue and vallecula on left side and abuts the anterior tonsillar pillar (long arrow)



**Figure 9:** Anteroposterior dimension: Axial three-dimensional image. Two perpendicular lines “a” and “b” drawn are the anterior and posterior tumor-mucosal junction, respectively. The length of the horizontal line “c” connecting these two perpendicular lines is considered as anteroposterior dimension which corresponds to T3 stage



**Figure 10:** Craniocaudal dimension: Postcontrast T1-weighted image (Coronal reformat). Two horizontal lines, “a,” “b,” were drawn on the superior and inferior tumor-mucosal junctions. A line “c” is drawn perpendicular to lines “a” and “b” through the middle of the tumor. The length of this line “c” represents the craniocaudal dimensions which correspond to T2 stage

clinical and histopathology staging assessments [Table 10]. Agreement for the N stage was poor ( $k = 0.091$ ) between the clinical and histopathology staging assessments [Table 11]. Mean depth of invasion by histology and MRI was 14.22 mm



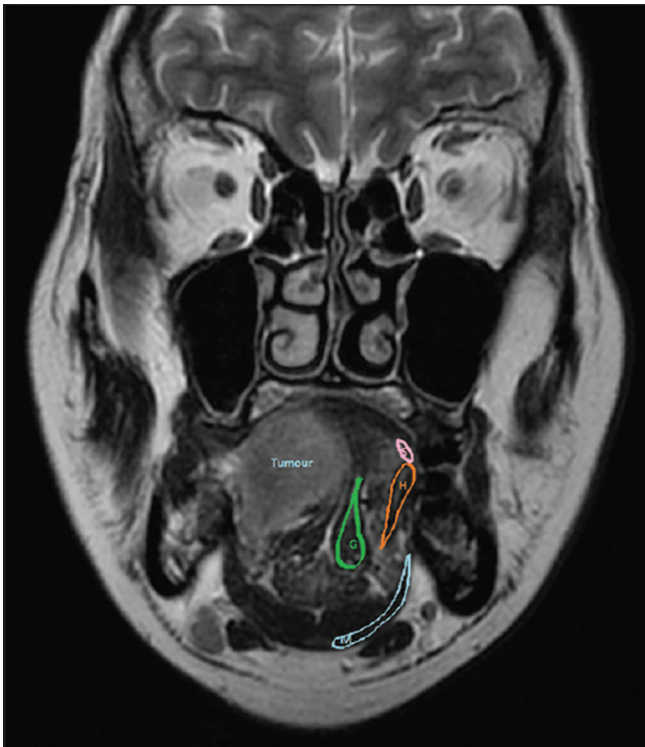


**Figure 11:** Coronal T2-weighted image demonstrating muscle invasion. Shows muscle invasion by the tumor. G = Genioglossus, H = Hyoglossus, S = Styloglossus, and M = Mylohyoid. Tumor on the right side shows the invasion of all muscles except mylohyoid

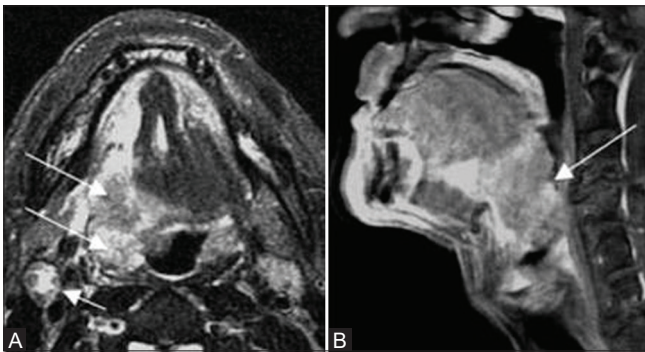


**Figure 13 (A and B):** (A) Axial T2 weighted fat-suppression image shows a right-sided tongue base cancer (T4aN2aM0-long arrows). An enlarged right jugulodigastric node is also seen (short arrow), the first echelon node of tongue base carcinoma. (B) Sagittal T2 weighted fat-suppression image of the same patient shows the extent of pharyngeal invasion of the tongue base tumor (arrow). Radiological DOI measured 13.2 mm and histopathological DOI measured 12.8 mm. MRI and histopathology assessments of tumor spread were equivalent to within 0.5 mm DOI

and 16.12 mm, respectively. Moderate agreement ( $k = 0.541$ ) was noted between clinical and pathological tumor depth [Table 12] and good agreement ( $k = 0.844$ ) was noted between radiological and pathological tumor depth [Table 13]. The correlation between depth of invasion reported on MRI and pathological depth of invasion ( $r = 0.93$ ;  $P < 0.001$ ).

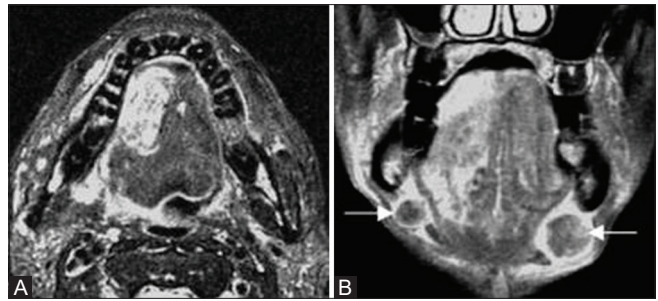


**Figure 12 (A and B):** (A) Axial T2 weighted fat-suppression image shows a right-sided tongue cancer (T1N1M0) extending more than 5 mm from the lateral margin of the tongue. (B) Coronal T2 weighted fat-suppression image shows bilateral submandibular lymphadenopathy (arrows), a result of the lymphatic drainage pathways of the inner two-thirds of the oral tongue. Radiological depth of invasion (DOI) measured 3.5 mm and histopathological DOI measured 3.2 mm. MRI and histopathology assessments of tumor spread were equivalent to within 0.5 mm DOI

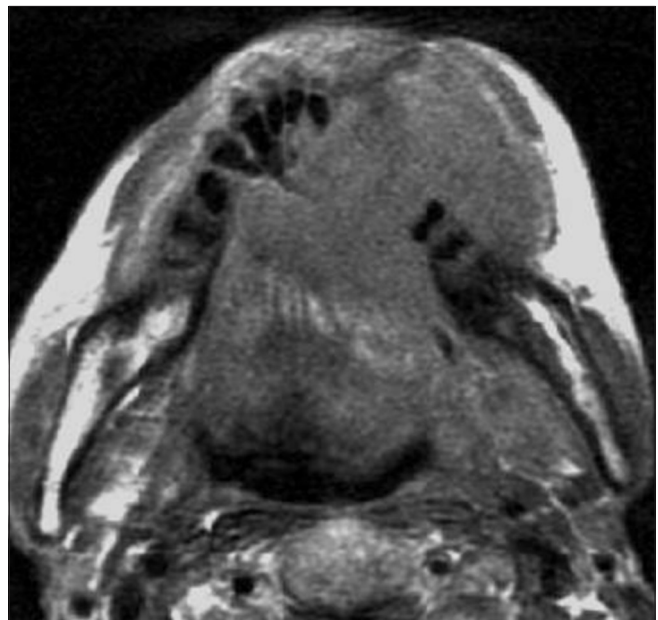


**Figure 14:** Axial T1 weighted image shows a tongue cancer (T4aN2aM0) with mandible invasion. However, the early involvement of cortical bones is better seen on CT images. Radiological DOI measured 14.4 mm and histopathological DOI measured 14.1 mm. MRI and histopathology assessments of tumor spread were equivalent to within 0.5 mm DOI

**Cutoff values for histopathological (HP) depth and MRI depth**

The cutoff value of HP depth that could determine the existence of nodal metastasis was 8 mm. The cutoff value for T1WGd MRI depth was 5 mm. With the HP depth cutoff value of 5 mm as a standard, groups were subdivided into those >5 mm and those <5 mm; the nodal metastasis rates for each group were 52% and 24%, respectively ( $P = 0.040$ ).

**Correlation between histopathological (HP) depth and MRI depth**

Pearson's correlation coefficient of HP depth and T1WGd MRI depth was 0.851 ( $P < 0.001$ ) suggesting that HP depth shows a strong correlation with T1WGd MRI depth.

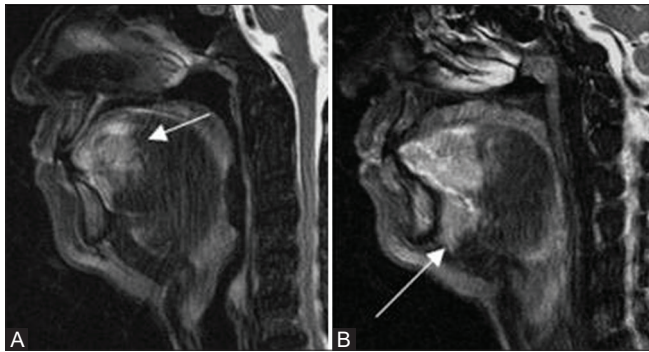


**Figure 15 (A and B):** (A) Sagittal T2 weighted fat-suppression image shows carcinoma in the anterior third of the oral tongue (T4aN1M0-arrow). (B) Sagittal T2 weighted fat-suppression image (same patient) shows tumor invading the floor of the mouth (arrow). Radiological DOI measured 13.2 mm and histopathological DOI measured 12.9 mm. MRI and histopathology assessments of tumor spread were equivalent to within 0.5 mm DOI

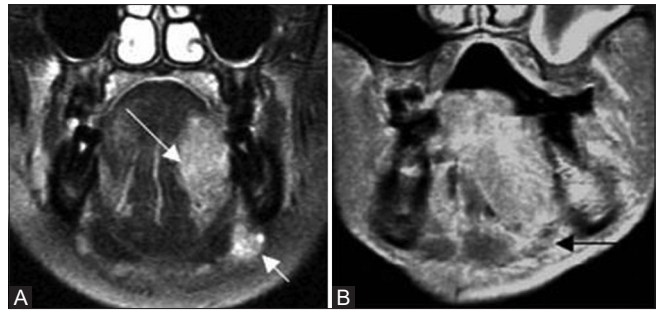


**Figure 16 (A and B):** (A) Coronal T2 weighted fat-suppression image shows a carcinoma in the middle third of the oral tongue (T3N1M0) with early infiltration (long arrow) of the tongue musculature (genioglossus). Note the ipsilateral submandibular lymphadenopathy (short arrow). (B) Coronal post-contrast T1 weighted fat-suppression image of a more advanced case shows the tumor invading the lateral floor of the mouth (T4aN1M0-arrow). Radiological DOI measured 9.2 mm and histopathological DOI measured 8.8 mm. MRI and histopathology assessments of tumor spread were equivalent to within 0.5 mm DOI

**Table 7: Correlation between MRI and clinical nodal (N) staging**

Clinical "N" staging	MRI "N" staging			Total
	N0	N1	N2	
N0	6	3	4	13
N1	0	6	6	12
N2	0	0	5	5
Total	6	9	15	30
Sensitivity	93.7%			
Specificity	95.2%			
PPV	93.8%			
Kappa coefficient	0.218, 95% CI (0.347-1.00)			

By applying the Chi-square test and kappa statistics, *P* and *k* come out to be 0.03 and 0.218, respectively, which shows fair agreement between the clinical and MRI staging assessments

**Table 8: Correlation between MRI and histopathological tumor (T) staging**

MRI "T" staging	HPE "T" staging				Total
	T1	T2	T3	T4	
T1	1	0	0	0	1
T2	0	10	0	0	10
T3	0	4	3	0	7
T4	0	4	4	4	12
Total	1	18	7	4	30
Sensitivity	94.2%				
Specificity	96.1%				
PPV	92%				
Kappa coefficient	0.822, 95% CI (0.631-1.00)				

By applying the Chi-square test and kappa statistics, *P* and *k* come out to be 0.01 and 0.822, respectively, which shows good/substantial agreement between the clinical and MRI staging assessments

## Discussion

In the current study, the extent of primary tumor (T) and metastasis to regional lymph nodes (N) was initially evaluated by clinical examinations followed by MR

imaging. The final diagnosis was made by histopathological examination (HPE). Kappa Index was used for data analysis which showed moderate agreement (kappa value 0.512) between the clinical and MRI "T" staging. This is consistent with the studies performed by Paiva *et al.*<sup>[20]</sup> and Hirunpat *et al.*<sup>[21]</sup> which also showed that mis-staging by clinical examination in the overall stage grouping was high. Also, there was good agreement (kappa value 0.822) for the T staging (tumor depth and width) between MRI and HPE assessments. The final staging assessed by MR imaging in the current study remains the same in 30 patients who underwent surgery and final staging by HPE. These results are consistent with the study conducted by Tetsumura *et al.*<sup>[22]</sup> in which the tumor depth and width were measured on both MR images and HPE and the authors observed a high correlation between the values measured by MRI and HPE.

In this study, clinical examination and MRI were both adequate at determining depth of invasion compared with final pathology when tumors were  $\geq 5$  mm in depth, but not for those less than 5 mm. We used 5 mm as a cutoff as this is the depth at which the risk of nodal metastases increases, based on the literature.<sup>[13,23]</sup> Since the clinical importance is to be able to detect deeper tumors, the decreased ability of either examination to be able to accurately predict the depth of superficial lesions is less clinically significant.

There have been previous studies investigating the accuracy of MRI in predicting the depth of invasion of oral tongue SCC; however, these studies primarily have a small sample size and retrospective study design, and none have compared MRI with clinical examination. Preda *et al.* investigated 33 oral tongue SCC in a retrospective series.<sup>[24]</sup> The authors demonstrated that MRI thicknesses correlated



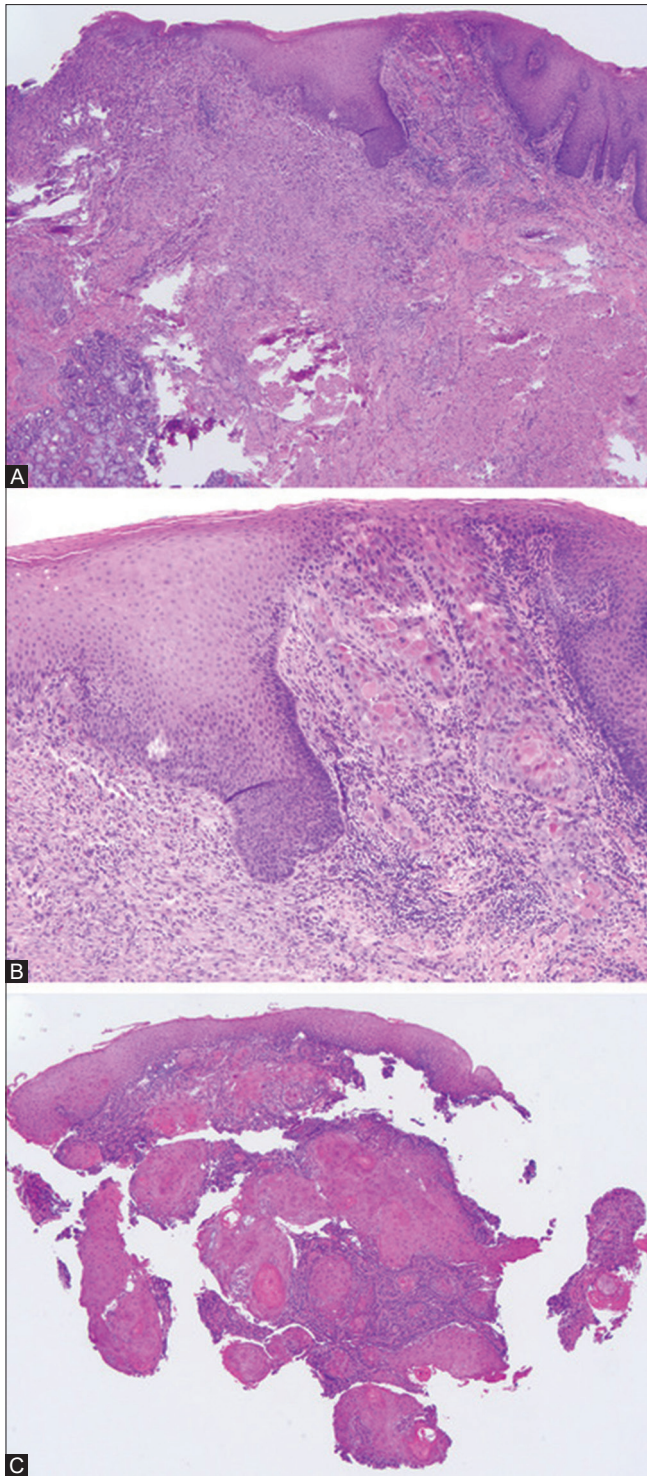


**Figure 17 (A-C):** (A) An example of minimal residual squamous cell carcinoma of the oral tongue (hematoxylin and eosin (H and E), original magnification  $\times 40$ ). (B) A minute focus of residual squamous cell carcinoma, about 1mm wide and 1mm deep, with submucosal scar in the left lower corner (H and E, original magnification  $\times 100$ ). (C) The diagnostic biopsy was represented by five tissue fragments, all of which were smaller than 5mm in greatest dimension and had invasive squamous cell carcinoma. The exact measurement of the depth of invasion in this case is difficult given the fragmented nature of diagnostic biopsy. Only one biopsy fragment had normal squamous mucosa allowing measurement of the depth of invasion (H and E, original magnification  $\times 40$ )

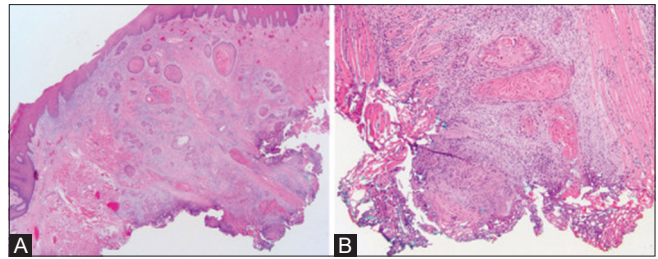


**Figure 18 (A and B):** An example of a T2 squamous cell carcinoma of the oral tongue with positive deep margin, indicating that the depth of invasion may be underestimated. (A) The apparent depth of invasion is 7mm; however, the deep margin is involved by carcinoma (hematoxylin and eosin (H and E), original magnification  $\times 20$ ). (B) Carcinoma at deep margin. Hypothetically, if there is additional 4mm (along the “plumb line”) of residual carcinoma in the tumor bed, this carcinoma is more appropriately staged as T3 (H and E, original magnification  $\times 100$ )

**Table 9: Correlation between MRI and histopathological (N) staging**

MRI “N” staging	HPE “N” staging			Total
	N0	N1	N2	
N0	5	0	0	5
N1	5	3	2	10
N2	4	3	8	15
Total	14	6	10	30
Sensitivity		94.3%		
Specificity		95.1%		
PPV		93%		
Kappa coefficient		0.931, 95% CI (0.751-1.00)		

By applying the Chi-square test and kappa statistics, *P* and *k* come out to be 0.01 and 0.931, respectively, which shows good agreement between the clinical and MRI staging assessments

**Table 10: Correlation between clinical and histopathological tumor (T) staging**

Clinical “T” staging	HPE “T” staging				Total
	T1	T2	T3	T4	
T1	4	0	0	0	4
T2	0	9	2	0	11
T3	0	5	1	2	8
T4	0	3	1	3	7
Total	4	17	4	5	30

By applying the Chi-square test and kappa statistics, *P* and *k* come out to be 0.01 and 0.012, respectively, which shows poor agreement between the clinical and MRI staging assessments

strongly with histological tumor thicknesses (correlation coefficient = 0.68, *P* < 0.0001). Park *et al.*<sup>[25]</sup> evaluated 114 patients with oral cavity and oropharyngeal SCC of which 49 patients had oral tongue SCC. Relationship between MRI and histologic depth of invasion in oral tongue subsite was high with a correlation coefficient of 0.949. In the current study, the mean depth of invasion by histology and MRI was 14.2 mm and 16.1 mm, respectively. This group reported on deeper tumors, explaining the better correlation.



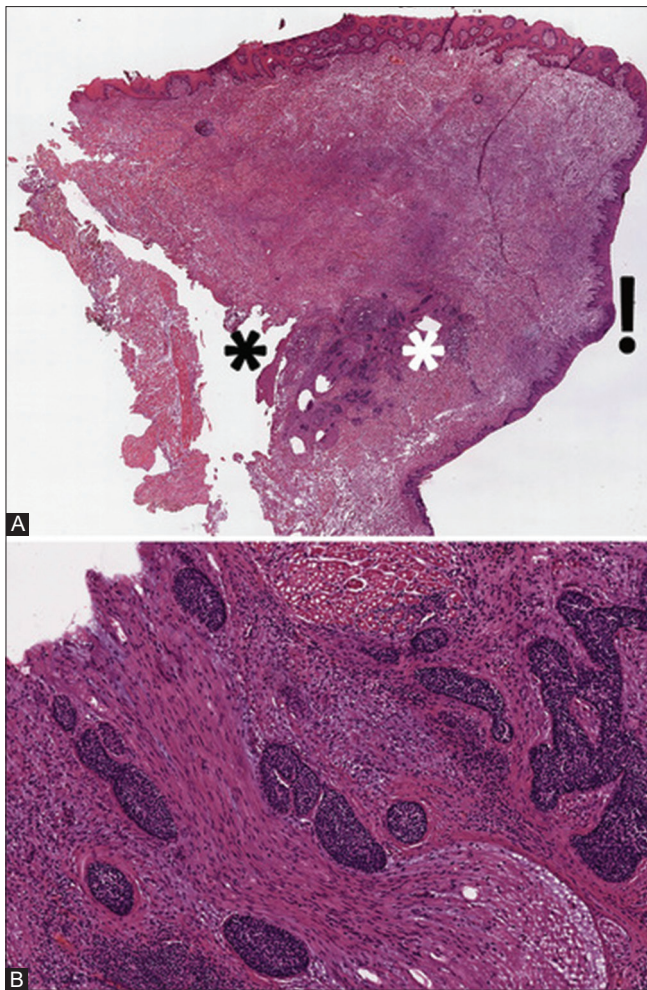


**Figure 19 (A and B):** Cross-section through left partial glossectomy with dorsal, lateral, and ventral (toward floor of mouth) mucosa (clockwise, starting from the top). (A) The focus of residual squamous cell carcinoma (between the white and black asterisks) shows no connection to mucosa. (B) Residual carcinoma is represented by foci of extensive perineural invasion. The potential reference points to measure the depth of invasion are along the dorsal, lateral, and ventral mucosa. On this section, depth of invasion was measured from the lateral mucosa (next to exclamation mark), because this area showed a focus of moderate-to-severe dysplasia. Hematoxylin and eosin, frozen section, images taken from the scanned whole slide image with original magnification of  $\times 1.2$

As pointed out by Lwin *et al.*,<sup>[26]</sup> there is tumor shrinkage after resection affecting all oral cavity subsites, including the oral tongue. The tumor shrinkage factor for oral tongue cancer has been reported to be 87%. Most of the studies assessing the relationship between tumor depth of invasion and risk of nodal metastases are based on pathologic assessment and not clinical or radiographic assessment. Therefore, clinical and MRI examination may under or over estimate depth of invasion and may not have the same ability to predict nodal metastases.

Sentinel lymph node (SLN) biopsy has been evaluated in recent years in head and neck cancer. A few studies evaluated SLN for oral and oropharyngeal cancer; however,

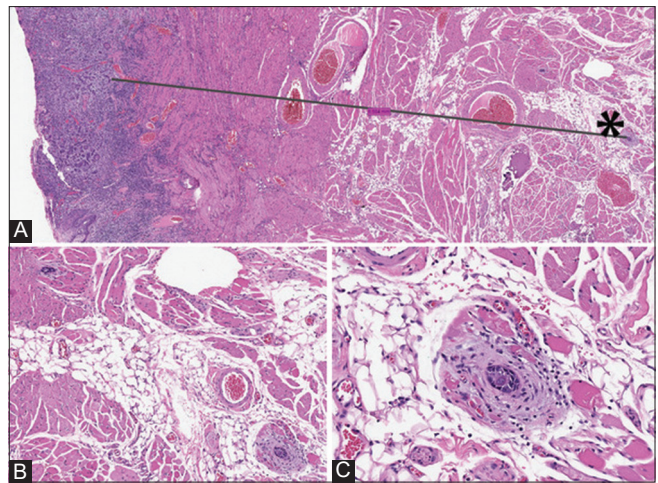


**Figure 20 (A-C):** (A) Two clusters of invasive squamous cell carcinoma (each with about 15 cells, by the black asterisk and in B and C) were 6.5 mm from the bulk of the tumor, suggestive of lymphatic invasion and representing the deepest point of invasion. The black line illustrates the way the distance between the invasive tumor front and remote foci of carcinoma was measured. The T1 stage was assigned based on the depth of invasion by the bulk of the tumor which was 4.5 mm. (B) One of the small clusters of carcinoma is in the left upper corner and the second focus of carcinoma is in the right lower corner. (C) Hematoxylin and eosin, images taken from the scanned whole slide image with original magnification of  $\times 1.2$

**Table 11: Correlation between clinical and histopathological (N) staging**

Clinical "N" staging	HPE "N" staging			Total
	N0	N1	N2	
N0	6	0	2	8
N1	6	5	4	15
N2	3	0	4	7
Total	15	5	10	30

By applying the Chi-square test and kappa statistics,  $P$  and  $k$  come out to be 0.01 and 0.091, respectively, which shows poor agreement between the clinical and MRI staging assessments

most of these studies included advanced T stage and did not study specific subsite.<sup>[27-29]</sup> Sagheb *et al.* did a pilot study to examine the role of SLN in early T stage tongue SCC with N0 neck. A SLN was followed by a neck dissection during the same operation.<sup>[30]</sup> It was concluded that the sensitivity of SLN is about 75% and further investigation is needed.

While MRI was shown to correlate well with pathological depth and is more sensitive and specific for depth measurements than clinical assessment, the latter test is complementary and useful in situations where either MRI is unavailable or difficult to interpret due to artefacts. In a prospective study, Yuen *et al.*<sup>[31]</sup> examined the correlation between ultrasound and pathologic tumor thickness in 45 oral tongue carcinoma patients during general anesthesia and before commencing surgery. There was a statistically significant correlation coefficient of 0.940 ( $P < .005$ ). While this technique may be difficult to perform in clinic due to



**Table 12: Sensitivity and specificity of clinical depth in comparison to pathological depth**

Clinical depth (mm)	Pathological depth (mm)		
	<5	>5	Total
<5	11	3	14
>5	5	11	16
Total	16	14	30
Sensitivity	-		70%
Specificity	-		78.5%
PPV	-		70%
Kappa coefficient	-	0.541, 95% CI (0.327-0.807)	

Kappa coefficients were used to determine the agreement between measures once categorized according to the cutoff point. Closer values to 1 mean higher agreement between categories.

**Table 13: Sensitivity and specificity of radiological depth in comparison to pathological depth**

Radiological depth (mm)	Pathological depth (mm)		
	<5	>5	Total
<5	14	1	15
>5	2	13	15
Total	16	14	30
Sensitivity	-		90%
Specificity	-		92.8%
PPV	-		90%
Kappa coefficient	-	0.844, 95% CI (0.563-1.00)	

Kappa coefficients were used to determine the agreement between measures once categorized according to the cutoff point. Closer values to 1 mean higher agreement between categories.

pain or trismus, its improved ability to measure tumor thickness does warrant further investigation. Despite the importance of depth of invasion, other histopathological parameters have been found to correlate with nodal metastasis including size of the tumor in greatest dimension, and other pathologic features such as pattern of invasion, density of cancer-associated fibroblasts, and perineural and vascular invasion.<sup>[32]</sup> All these need to be taken in account to determine the risk of regional metastasis.

Multiple pulse sequences had been used in the previous works to detect small tongue carcinoma and accurately identify tumor margins, including T2WI, STIR, and T1-weighted fat-suppressed contrast-enhanced sequences. Lam *et al.*<sup>[33]</sup> reported that particularly contrast-enhanced T1-weighted MRI provides a satisfactory accurate correlation between MRI tumor thickness and histologic tumor thickness in oral tongue cancer. Background diffusion-weighted imaging obtained with magnetic resonance (DW-MRI) is a noninvasive imaging tool potentially able to provide information about micro-structure tumor characteristics. The inclusion of DWI/ADC values might be helpful for differentiation between true tumor margin and edema, and also for distinction between benign and malignant head and neck tumors. Multiple studies reported high

diagnostic accuracy of DWI for differentiation of malignant from benign status of metastatic cervical lymph nodes.<sup>[34]</sup>

There are several studies<sup>[35]</sup> which tested the reliability of MRI in measuring tongue tumor thickness and correlated it well with histologic tumor thickness. Spiro *et al.*<sup>[36]</sup> postulated that disease-related death is apparently unusual when oral tumors are thin, regardless of tumor stage, and that tumor thickness rather than stage may have the best correlation with treatment failure and survival. However, tongue carcinoma may vary in shape and growth pattern. Therefore, depth of invasion (represented by para-lingual distance), not merely tumor thickness, is another important prognostic factor.

The current study evaluated the clinical assessment of tumor thickness in comparison to radiographic interpretation. There are strong correlations between pathological, radiological, and clinical measurements. Specifically, for oral tongue, cut-off of 5mm has been suggested. Finally, just where to measure DOI from can be difficult to determine in oral tongue (with mucosa on dorsal, lateral, and ventral aspects) and in undulating hyperplastic epithelium, which can create an uneven basement membrane. One has to imagine an arcuate reference line and then drop a “plumb-line” which can be equally as difficult due to variations in normal mucosa and DOI at different tumor section. The study highlighted the potential impact on T staging of extratumoral foci of SCC due to perineural invasion. It must be noted that a large proportion of extratumoral NI or LI occurs in tumors that are already T3, thus diminishing their impact on staging. Extratumoral perineural invasion represents a challenge to DOI measurement in isolated cases only. These scenarios are not currently directly addressed in the AJCC 8<sup>th</sup> edition description of DOI. However, they are covered under a more general TNM principle: when in doubt, the less advanced attribute should be selected (i.e., smaller DOI measurement, not including the extratumoral perineural invasion).

The oral tongue is covered by mucosa on its dorsal, lateral, and ventral aspects and a simple “plumb line” method may be difficult to apply in some cases. When residual carcinoma is small and not connected to the mucosal surface, the reference point from which to measure the DOI is perhaps best represented by mucosa with squamous dysplasia. In oral tongue, the level of the basement membrane of the closest adjacent normal mucosa is probably better represented by an arcuate rather than a straight line, especially when the line is drawn through two points, i.e., normal mucosa on both sides of carcinoma.

The current study showed that in up to 12% of apparently T2 cases, DOI may be underestimated due to the positive deep margin. Rarely, extratumoral perineural invasion

may be the deepest point of invasion, but it is unlikely to affect T stage. DOI measurement for early SCC of the oral tongue may require re-examination of the diagnostic biopsy slides in up to 20% of cases due to the absence or only minimal residual carcinoma in glossectomy specimens. A proactive assessment and reporting of DOI on diagnostic biopsies or documentation of factors limiting DOI measurement (e.g., fragmentation, lack of normal mucosa, absence of intrinsic tongue musculature) may minimize the need to re-review the original diagnostic biopsy when the glossectomy reveals no or minimal residual carcinoma.

## Conclusion

MRI is the imaging modality of choice for evaluation of tongue carcinoma as MRI helps in the accurate staging of the tumor using TNM classification which is crucial for optimizing treatment options. The current study shows a high correlation between MRI and HPE findings regarding thickness of tumor and depth of invasion. MRI and histopathology assessments of tumor spread were equivalent to within 0.5 mm DOI. In conclusion, estimation of invasion depth using MRI as a preoperative study in oral tongue carcinoma is essential in planning surgical treatment strategies such as the extent of elective neck dissection. Invasion depth, which greatly affects occult node metastases, must be included in the TNM staging of oral tongue carcinoma.

## Limitations of the study

The limitations of our study include a relatively small number of cases and errors caused by manual measurement of tumor thickness during clinical examination.

## Declaration of patient consent

The authors certify that they have obtained all appropriate patient consent forms. In the form, the patients have given their consent for their images and other clinical information to be reported in the journal. The patients understand that their names and initials will not be published and due efforts will be made to conceal their identity, but anonymity cannot be guaranteed.

## Acknowledgement

The author would like to thank Mr. Rethesh, Senior Radiographer, Department of Radiology, Holy Family Hospital, Thodupuzha for the help rendered in the preparation of schematic diagrams and acquisition of MR images.

## Financial support and sponsorship

Nil.

## Conflicts of interest

There are no conflicts of interest.

## References

1. Newman AN, Rice DH, Ossoff RH, Sisson GA. Carcinoma of the tongue in persons younger than 30 years of age. *Arch Otolaryngol* 1983;109:302-4.
2. Goldenberg D, Ardekian L, Rachmiel A, Peled M, Joachims HZ, Laufer D. Carcinoma of the dorsum of the tongue. *Head Neck* 2000;22:190-4.
3. Flamant R, Hayem M, Lazar P, Denoix P. Cancer of the tongue. A study of 904 cases. *Cancer* 1964;17:377-85.
4. Coombes D, Cascarini L, Booth PW. Carcinoma of the midline dorsum of the tongue. *Br J Oral Maxillofac Surg* 2008;46:485-6.
5. Schwartzfeld T. Cancer of the posterior one-third of the tongue and the floor of the mouth: Present forms of treatment. *J Am Osteopath Assoc* 1975;74:1174-9.
6. Frazell EL, Lucas JC Jr. Cancer of the tongue. Report of the management of 1,554 patients. *Cancer* 1962;15:1085-99.
7. Rana M, Iqbal A, Warraich R, Ruecker M, Eckardt AM, Gellrich NC. Modern surgical management of tongue carcinoma-A clinical retrospective research over a 12 years period. *Head Neck Oncol* 2011;3:43.
8. Ng JH, Iyer NG, Tan M-H, Edgren G. Changing epidemiology of oral squamous cell carcinoma of the tongue: A global study. *Head Neck* 2017;39:297-304.
9. Nithya C, Pandey M, Naik B, Ahamed IM. Patterns of cervical metastasis from carcinoma of the oral tongue. *World J Surg Oncol* 2003;1:10.
10. Woolgar JA, Scott J. Prediction of cervical lymph node metastasis in squamous cell carcinoma of the tongue/floor of mouth. *Head Neck* 1995;17:463-72.
11. Farmer RW, McCall L, Civantos FJ, Myers JN, Yarbrough WG, Murphy B, *et al.* Lymphatic drainage patterns in oral squamous cell carcinoma: Findings of the ACOSOG Z0360 (Alliance) study. *Otolaryngol Head Neck Surg* 2015;152:673-77.
12. DiTroia JF. Nodal metastases and prognosis in carcinoma of the oral cavity. *Otolaryngol Clin N Am* 1972;5:333-42.
13. Fukano H, Matsuura H, Hasegawa Y, Nakamura S. Depth of invasion as a predictive factor for cervical lymph node metastasis in tongue carcinoma. *Head Neck* 1997;19:205-10.
14. Umeda M, Nishimatsu N, Teranobu O, Shimada K. Criteria for diagnosing lymph node metastasis from squamous cell carcinoma of the oral cavity: A study of the relationship between computed tomographic and histologic findings and outcome. *J Oral Maxillofac Surg* 1998;56:585-93.
15. Chiesa F, Mauri S, Grana C, Tradati N, Calabrese L, Ansarin M, *et al.* Is there a role for sentinel node biopsy in early N0 tongue tumours? *Surgery* 2000;128:16-21.
16. Ong CK, Chong VF. Imaging of tongue carcinoma. *Cancer Imaging* 2006;6:186-93.
17. Arakawa A, Tsuruta J, Nishimura R, Sakamoto Y, Korogi Y, Baba Y, *et al.* Lingual carcinoma: Correlation of MR imaging with histopathological findings. *Acta Radiol* 1996;37:700-7.
18. Bassi KK, Srivastava A, Seenu V, Kumar R, Parshad R, Chumber S, *et al.* The first and second echelon sentinel lymph node evaluation in oral cancer. *Indian J Surg* 2013;75:377-82.
19. Sobin LH, Wittekind C, editors. *UICC TNM Classification of Malignant Tumors*. 6<sup>th</sup> ed. New York: Wiley; 2002.
20. Paiva RR, Figueiredo PTS, Leite AF, Silv, MAG, Guerra ENS. Oral cancer staging established by magnetic resonance imaging. *Braz Oral Res* 2011;25:512-8.
21. Hirunpat S, Paiboon JJ, Angunsri N, Chowchuech V. When should MRI be recommended for the accurate clinical staging of base of tongue carcinoma. *Asian Pac J Cancer Prev* 2007;8:310-4.



22. Tetsumura A, Yoshino N, Amagasa T, Nagumo K, Okada N, Sasaki T. High-resolution magnetic resonance imaging of squamous cell carcinoma of the tongue: An *in vitro* study. *Dentomaxillofac Radiol* 2001;30:14-21.
23. Layland MK, Sessions DG, Lenox J. The influence of lymph node metastasis in the treatment of squamous cell carcinoma of the oral cavity, oropharynx, larynx, and hypopharynx: N0 versus N+. *Laryngoscope* 2005;115:629-39.
24. Preda L, Chiesa F, Calabrese L, Latronico A, Bruschini R, Leon ME, *et al.* Relationship between histologic thickness of tongue carcinoma and thickness estimated from preoperative MRI. *Eur Radiol* 2006;16:2242-8.
25. Park JO, Jung SL, Joo YH, Jung CK, Cho KJ, Kim MS. Diagnostic accuracy of magnetic resonance imaging (MRI) in the assessment of tumor invasion depth in oral/oropharyngeal cancer. *Oral Oncol* 2011;47:381-6.
26. Lwin CT, Hanlon R, Lowe D, Brown JS, Woolgar JA, Triantafyllou A, *et al.* Accuracy of MRI in prediction of tumour thickness and nodal stage in oral squamous cell carcinoma. *Oral Oncol* 2012;48:149-54.
27. Chone CT, Magalhes RS, Etchehebere E, Camargo E, Altemani A, Crespo AN. Predictive value of sentinel node biopsy in head and neck cancer. *Acta Otolaryngol* 2008;128:920-4.
28. Stoeckli SJ, Alkureishi LW, Ross GL. Sentinel node biopsy for early oral and oropharyngeal squamous cell carcinoma. *Eur Arch Otorhinolaryngol* 2009;266:787-93.
29. Kuriakose MA, Trivedi NP. Sentinel node biopsy in head and neck squamous cell carcinoma. *Curr Opin Otolaryngol Head Neck Surg* 2009;17:100-10.
30. Sagheb K, Sagheb K, Rahimi-Nedjat R, Taylor K, Al-Nawas B, Walter C. Sentinel lymph node biopsy in T1/T2 squamous cell carcinomas of the tongue: A prospective study. *Oncol Lett* 2016;11:600-4.
31. Yuen AP, Ng RW, Lam PK, Ho A. Preoperative measurement of tumor thickness of oral tongue carcinoma with intraoral ultrasonography. *Head Neck* 2008;30:230-4.
32. Almangush A, Bello IO, Keski-Säntti H, Mäkinen LK, Kauppila JH, Pukkila M, *et al.* Depth of invasion, tumor budding, and worst pattern of invasion: Prognostic indicators in early-stage oral tongue cancer. *Head Neck* 2013;21. doi: 10.1002/hed.23380.
33. Lam P, Au-Yeung KM, Cheng PW, Wei WI, Yuen AP, Trendell-Smith N, *et al.* Correlating MRI and histologic tumor thickness in the assessment of oral tongue cancer. *Am J Roentgenol* 2004;182:803-8.
34. Zhong J, Lu Z, Xu L, Wei WI, Yuen AP, Trendell-Smith N, *et al.* The diagnostic value of cervical lymph node metastasis in head and neck squamous carcinoma by using diffusion-weighted magnetic resonance imaging and computed tomography perfusion. *Biomed Res Int* 2014;2014:260859.
35. Bashir U, Manzoor MU, Majeed Y, Khan RU, Hassan U, Murtaza A, *et al.* Reliability of MRI in measuring tongue tumour thickness: A 1.5T study. *J Ayub Med Coll Abbottabad* 2011;23:101-4.
36. Spiro RH, Huvos AG, Wong GY, Spiro JD, Gnecco CA, Strong EW. Predictive value of tumor thickness in squamous carcinoma confined to the tongue and floor of the mouth. *Am J Surg* 1986;152:345-50.